

Numerical study of the lattice meson form factor

R. M. Woloshyn

TRIUMF, 4004 Wesbrook Mall, Vancouver, British Columbia, Canada V6T 2A3

A. M. Kobos

SuperComputing Services, The University of Calgary, Calgary, Alberta, Canada T2N 1N4

(Received 1 July 1985)

The electric form factor of the pseudo-Goldstone meson (the generic pion) is calculated in quenched lattice quantum chromodynamics with SU(2) color. Charge radii are calculated for different values of the bare-quark mass. The results are in agreement with the physically reasonable expectation that heavier quarks have distributions of smaller radius.

I. INTRODUCTION

Recently there has been considerable interest in determining lattice hadron sizes and internal structure.¹⁻⁴ The study of electromagnetic properties can be very useful for this purpose. In Ref. 1 the feasibility of a lattice calculation of the meson electric form factor was demonstrated. In Ref. 5 a detailed derivation of the lattice three-point function was given and it was shown how the form factor could be extracted from a combination of two- and three-point functions. In this paper we use the results of Ref. 5 in a numerical survey of the pseudoscalar-meson electric form factor as a function of quark mass.

The staggered scheme^{6,7} for putting fermions on the lattice is used. The interpretation of the staggered fermion degrees of freedom is usually made in terms of flavored quark fields defined on hypercubes in the lattice.⁸⁻¹⁰ The two-point function, needed for mass calculations, can be cast in a form that is constructed using only local combinations of staggered fermion fields.⁸⁻¹¹ In Ref. 5 it was shown that the electric form factor can be extracted from a three-point function which involves only local staggered-fermion-field bilinear operators as interpolating fields. The relevant formulas are reviewed in Sec. II.

Section III contains details of the numerical work and the results are given in Sec. IV. The calculations are done in a model with SU(2) color (at $\beta=2.3$) for five values of the bare-quark mass from $ma=0.025$ to $ma=0.4$. The meson masses we obtain agree very well with previous calculations. The electric form factor is calculated for a 0^- meson (pseudo-Goldstone boson) with an equal-mass quark-antiquark pair. The results show clearly that the charge radius decreases as the quark mass increases.

Pseudoscalar mesons with unequal-mass quarks and antiquarks are also considered. Allowing the charge-density operator to act either on the light or on the heavy quark gives information on their relative distribution. We obtain the physically reasonable result that, when the quarks have very different masses, the heavy quark has a much smaller charge radius than the light quark. This provides good evidence that our measurement is indeed probing the

meson structure.

Conclusions are given in Sec. V.

II. FORMALISM

In this paper we consider a charged pseudo-Goldstone meson (a generic pion) associated with the remnant continuous axial global symmetry present in the staggered scheme of lattice fermions.^{7,8} The usual flavor structure associated with the staggered fermions is not useful for constructing charged states since an "electric charge" defined within these flavors is not conserved.¹² We therefore introduce two sets of flavors, labeled by u and d , with charges q^u and q^d . The action takes the form (suppressing color indices)

$$S_F(U) = \bar{\chi} M \chi \tag{1a}$$

$$= \frac{1}{2} \sum_{x,\mu,f=\{u,d\}} \alpha_\mu(x) [\bar{\chi}^f(x) U_\mu(x) \chi^f(x+a_\mu) - \bar{\chi}^f(x+a_\mu) U_\mu^\dagger(x) \chi^f(x)] + ma \sum_{x,f} \bar{\chi}^f(x) \chi^f(x), \tag{1b}$$

where

$$\alpha_\mu(x) = (-1)^{\xi_\mu}, \quad \xi_\mu = \sum_{\nu < \mu} x_\nu.$$

A conserved vector current can be derived using the Noether procedure.^{7,8} The result is (for each species, $f=u,d$)

$$j_\mu^f(x) = \frac{-i}{2} \alpha_\mu(x) [\bar{\chi}^f(x) U_\mu(x) \chi^f(x+a_\mu) + \bar{\chi}^f(x+a_\mu) U_\mu^\dagger(x) \chi^f(x)]. \tag{2}$$

The usual way to expose the particle content of the staggered-fermion theory is to construct nonlocal quark fields defined on hypercubes in the lattice. This is discussed in detail in many papers.⁸⁻¹¹ The end result is that the two-point function [which is essentially the correlation function of the local interpolating field $\alpha_4(x) (-1)^t \bar{\chi}^d(\mathbf{x}, t) \chi^u(\mathbf{x}, t)$]

$$G_0(\mathbf{p};t) \equiv \frac{1}{N_c} \sum_{\mathbf{x},c} e^{-i\mathbf{p}\cdot\mathbf{x}} \text{Tr} M^{-1}(\mathbf{x},t;0) [M^{-1}(\mathbf{x},t;0)]^\dagger, \quad (3)$$

where the trace implies a sum over appropriate color and

flavor indices, describes the propagator of a 0^- pseudo-Goldstone meson. The sum c is over Monte Carlo lattice gauge field configurations (N_c in number). We also use the correlation function in the $J=1$ channel

$$G_1(\mathbf{p};t) \equiv \frac{1}{N_c} \sum_{\mathbf{x},c} e^{-i\mathbf{p}\cdot\mathbf{x}} [(-1)^{x_1} + (-1)^{x_2} + (-1)^{x_3}] \text{Tr} M^{-1}(\mathbf{x},t;0) [M^{-1}(\mathbf{x},t;0)]^\dagger. \quad (4)$$

This describes the propagation of vector and axial-vector mesons.

In Ref. 5 it was shown that the matrix element of the charge-density operator between pion states could be extracted from the lattice three-point function

$$A(\mathbf{p},\mathbf{q};t_2,t_1) = \sum_{\mathbf{x}_2} e^{-i\mathbf{p}\cdot\mathbf{x}_2} \alpha_4(\mathbf{x}_2) (-1)^{t_2} \langle \bar{\chi}^d(\mathbf{x}_2,t_2) \chi^u(\mathbf{x}_2,t_2) \sum_{\mathbf{x}_1} e^{i\mathbf{q}\cdot\mathbf{x}_1} \rho(\mathbf{x}_1,t_1) \bar{\chi}^u(0) \chi^d(0) \rangle, \quad (5)$$

where

$$\rho(\mathbf{x},t) = \sum_f q^f j_4^f(\mathbf{x},t).$$

Notice that this three-point function just involves local interpolating fields.

The most convenient way to determine the electric form factor from the Monte Carlo data is to take the combination

$$\mathcal{R} = \left[\frac{A(0,\mathbf{q};t_2,t_1) A(\mathbf{q},\mathbf{q};t_2,t_1)}{G_0(0;t_2) G_0(\mathbf{q},t_2)} \right]^{1/2} \xrightarrow{0 \ll t_1 \ll t_2} \frac{E_q + M_0}{2(E_q M_0)^{1/2}} F(q), \quad (6)$$

where the electric form factor¹³ is defined by

$$\langle \pi^+(p) | \rho(0) | \pi^+(p') \rangle = (E_p + E_{p'}) F(q). \quad (7)$$

III. COMPUTATIONAL DETAILS

Numerical calculations were done in a model for QCD using only SU(2) color. The lattice size was $10^2 \times 20 \times 16$ with the current-carrying momentum in the 3 direction. Twenty gauge-field configurations, prepared with the heat-bath Monte Carlo method¹⁴ in quenched approximation, were used. The gauge fields were constructed using the Wilson gauge-field action¹⁵ at $\beta=2.3$ on a $10^3 \times 16$ lattice and then doubled in the 3 direction.

Fermion propagators were calculated using the conjugate gradient algorithm.¹⁶ Iterations were carried out until the maximum change in the correlation function $G_0(0;t)$ at any time point was less than 0.05% in four iterations. The absolute value squared of the residual vectors was less than 10^{-11} to 10^{-10} . These calculations required about 5 CPU hours on a two-pipe Cyber 205 using full-precision arithmetic.

Antiperiodic boundaries were used on fermion fields in the spatial directions. However, the fermion coupling was put equal to zero across the time boundary of the lattice. The advantage of this choice is that correlation functions have a simple exponential falloff at large time separation. Furthermore, charge conservation takes a very simple form. The disadvantage of our boundary condition is that nonvacuum contributions can contaminate matrix elements when operators are placed near the time edges.¹⁷ Fortunately the combination \mathcal{R} of Eq. (6) removes all the time dependence and the factors that refer to the time boundary. We expect the form factor extracted using Eq. (6) to be free of time-boundary effects.

The three-point function was calculated as the derivative of a two-point function with the charge operator acting as a source.^{5,18} A check of this procedure was made at $q=0$ where the three- and two-point functions are related.¹⁹ It indicates that, at the lightest quark mass, our derivative is accurate to within 2–3% and becomes better when the quark mass is increased.

The standard statistical error was calculated at each time value of the two-point functions using the whole sample of 20 configurations. Meson masses were determined by fitting $G(0;t)$ with ae^{-bt} for times three through ten steps removed from the hadron creation operator. The uncertainty in the mass was determined from the error matrix of the least-squares fit. Statistical errors in the combination of three- and two-point functions \mathcal{R} were calculated including covariances between the different factors.²⁰ Again all 20 configurations were included in a single sum. The form factor was obtained from an average (weighted by statistical errors) of \mathcal{R} for times five through nine steps from the initial-hadron creation operator. The charge-density operator is placed at time step four; i.e., it acts between times steps four and five.

IV. RESULTS

The pseudoscalar-meson masses $M_0 a$ for an equal-mass quark and antiquark are shown in Fig. 1 as a function of bare-quark mass ma . The mass in the $J=1$ channel is also shown. This was obtained by fitting the two-point function $G_1(0,t)$ with a single exponential, essentially ig-

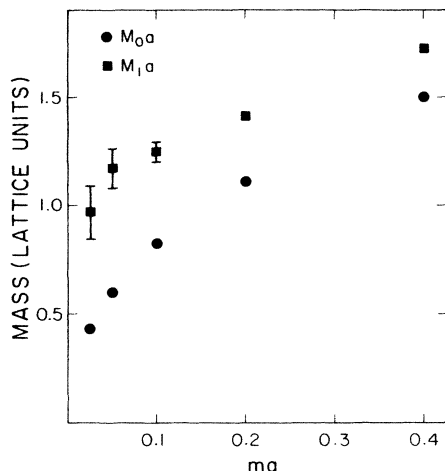


FIG. 1. Pseudoscalar- (●) and vector- (■) meson masses versus the bare-quark mass.

noting a small admixture of 1^+ state. Although this is an approximation it should be adequate for our purposes. Where we can make a direct comparison (at $ma=0.1, 0.2$) our pseudoscalar and vector masses agree very well with those of Billoire, Lacaze, Marinari, and Morel.¹¹

In Fig. 2 we plot $M_0^2 a^2$ versus the bare-quark mass ma . If PCAC (partial conservation of axial-vector current) holds this relation should be linear with $M_0^2 a^2$ extrapolating to zero at zero quark mass.²¹ Indeed, we find that these conditions are satisfied at the smaller values of quark mass. The line is not a fit but is a guide for the eye.

Figure 3 shows a typical result for the combination of three- and two-point functions \mathcal{R} of Eq. (6) versus the

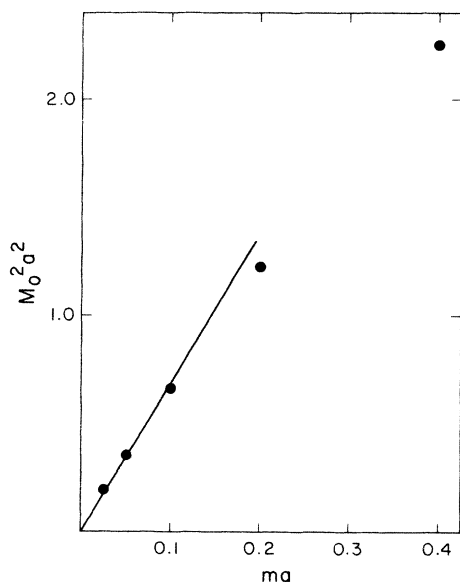


FIG. 2. Square of the pseudoscalar-meson mass versus the bare-quark mass.

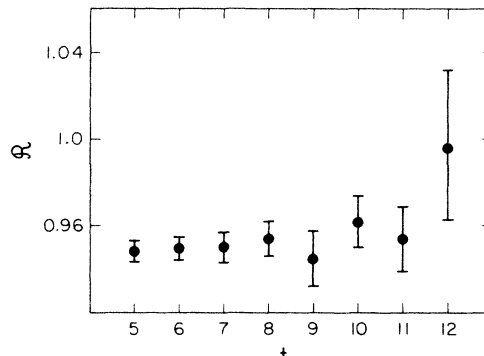


FIG. 3. The combination \mathcal{R} of three- and two-point functions [Eq. (6)] versus the time coordinate of the meson annihilation operator. The charge-density operator acts between time step 4 and 5.

time t_2 at which the hadron annihilation operator acts. The charge-density operator acts at time $t_1=4$. When $t_2 < t_1$, \mathcal{R} is zero to within a few percent. This reflects current conservation and the fact that with our time-boundary conditions there is a net charge present only for times between the action of the meson creation ($t=0$) and annihilation operators ($t=t_2$).

The electric form factor of the pseudoscalar meson was calculated at two values of momentum transfer, for $q=\pi/10$, the lowest-momentum value on our lattice, and for $q=\pi/5$. The results plotted as a function of Minkowskian four-momentum transfer squared $Q^2=2M_0(q^2+M_0^2)^{1/2}$ (in lattice units) are shown in Fig. 4. We see clearly that large quark masses lead to a more slowly decreasing form factor. This can be seen again in Fig. 5(a) where the form-factor values at $q=\pi/10$ are plotted as a function of quark mass. To extract a root-mean-square radius R_{rms} the form-factor values at $q=\pi/10$ are first parametrized using $F(Q^2)=(1+Q^2 a^2/\lambda^2)^{-1}$ then the relation $R_{\text{rms}}^2=-6dF/dQ^2$ is used on the monopole fit.²² The resulting charge radii are shown in Fig. 5(b). The parameters λ^2 themselves show an interesting behavior. They are plotted in Fig. 6 as a function of quark mass. Also shown are the values of $\lambda^2/M_1^2 a^2$, which within errors are constant, although not equal to one. The idea

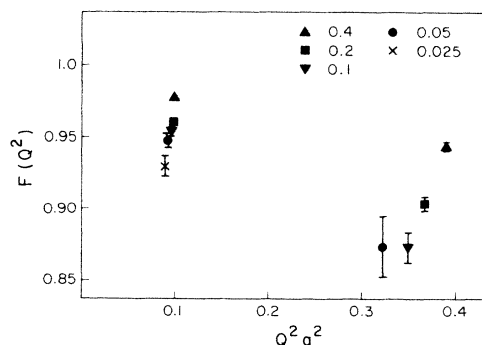


FIG. 4. The pseudoscalar-meson electric form factor versus Minkowskian four-momentum transfer squared $Q^2 a^2$ for different values of the quark mass from $ma=0.025$ to $ma=0.4$.

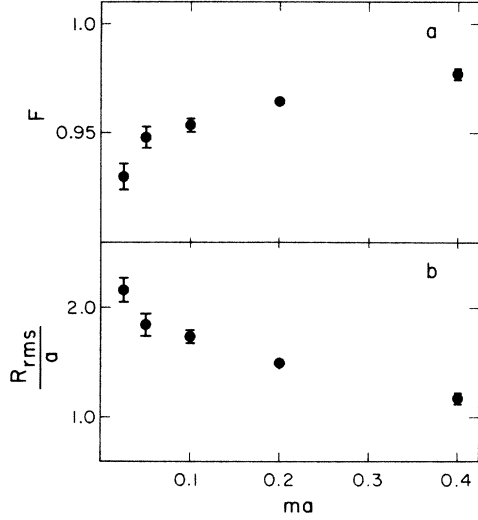


FIG. 5. (a) The pseudoscalar-meson electric form factor at $q = \pi/10$ versus the quark mass. (b) The meson root-mean-square radius R_{rms} versus the bare-quark mass.

that the low-momentum-transfer falloff of form factors is intimately related to vector mesons is an old one²³ and it is amusing that, to some extent, we observe a connection in our calculations.

The above calculations were done keeping quarks with different flavors degenerate in mass. It is also interesting to consider the situation where one quark has a mass very different from the other. We have done a calculation for pseudoscalar mesons in which one of the quark masses is

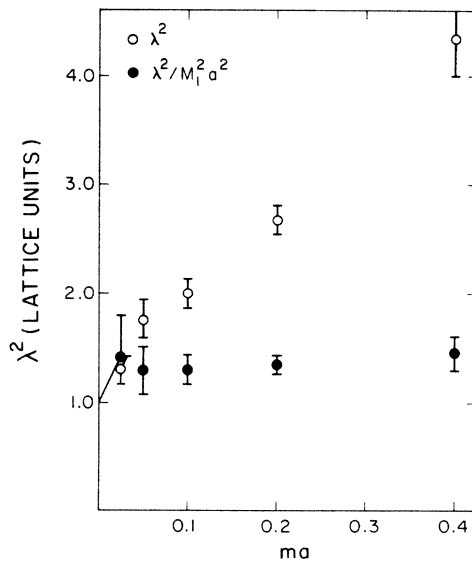


FIG. 6. The λ^2 parameter from a monopole parametrization of the electric form factor versus the quark mass. The quantity λ^2 is shown both in lattice units (\circ) and divided by the vector-meson mass squared (\bullet).

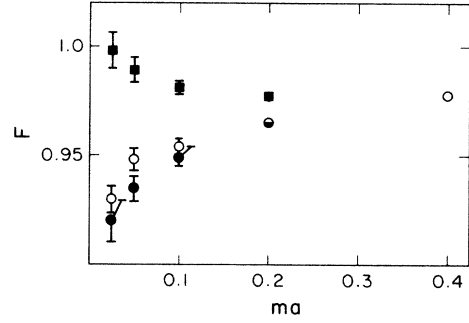


FIG. 7. The electric form factor for the light (\bullet) and heavy (\blacksquare) quark at $q = \pi/10$ of a pseudoscalar meson with an unequal-mass quark-antiquark pair versus the light-quark mass. The heavy-quark mass is fixed at $ma = 0.4$. For comparison the meson form factor in a meson with an equal-mass quark-antiquark pair (\circ) is also shown.

fixed at $ma = 0.4$ and the other is allowed to decrease to $ma = 0.025$. Form factors are calculated with the charge-density operator acting either on the light or on the heavy quark. The results at one unit of momentum transfer ($q = \pi/10$) are shown in Fig. 7. The form factor of the lighter quark essentially tracks the form factor of a meson with a light quark-antiquark pair. The form factor of the (fixed-mass) heavy quark approaches unity as the light-quark mass decreases. Parametrizing these form factors with monopoles and extracting the root-mean-square radius yields the results of Fig. 8. We observe the physically reasonable result that in a meson with unequal-mass quarks the distribution of the heavy quark has a smaller radius than the distribution of the light quark. This is good evidence that our form factor is really reflecting the meson structure and is not, for example, an artifact of the finite lattice.

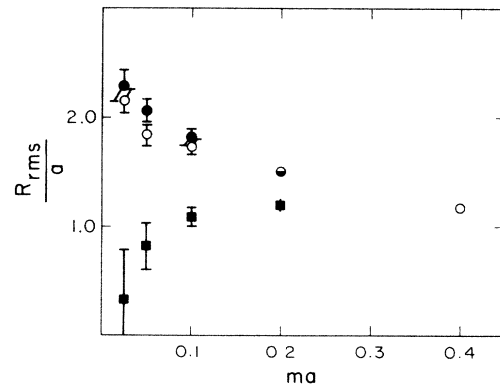


FIG. 8. The root-mean-square radius R_{rms} for the light (\bullet) and heavy (\blacksquare) quark in a pseudoscalar meson with an unequal-mass quark-antiquark pair versus the light-quark mass. The heavy-quark mass is fixed at $ma = 0.4$. For comparison the root-mean-square radius of a meson with an equal-mass quark-antiquark pair (\circ) is also shown.

V. CONCLUSION

In this paper we have done a survey of the 0^- lattice meson (pseudo-Goldstone boson) electric form factor as a function of quark mass. The staggered scheme for lattice fermions was used and calculations were done in a model for quenched lattice QCD with SU(2) color.

The results clearly show that the meson charge radius decreases as the quark mass increases. Parametrizing the form factor at low momentum transfer with a monopole $(1 + Q^2 a^2 / \lambda^2)^{-1}$ we find that the parameters λ^2 are proportional to the vector-meson mass squared, reminiscent of vector-dominance ideas. The constant of proportionality is not however equal to one.

The form factor for pseudoscalar mesons with an unequal-mass quark-antiquark pair has also been calculat-

ed. Allowing the charge-density operator to act either on the light or on the heavy quark shows that the distribution of the heavy quark has a smaller radius than that of the light quark. This result gives us considerable confidence that the form factor we calculate is reflecting the meson structure correctly.

The extension of the form-factor calculations to SU(3) color and the baryon sector would be very interesting and, ultimately, could provide one of the best quantitative tests of QCD.

ACKNOWLEDGMENTS

We thank SuperComputing Services at the University of Calgary for providing time on the Cyber 205 computer. This work was supported in part by the Natural Sciences and Engineering Research Council of Canada.

-
- ¹W. Wilcox and R. M. Woloshyn, Phys. Rev. Lett. **54**, 2653 (1985).
²B. Velikson and D. Weingarten, Nucl. Phys. **B249**, 433 (1985).
³O. Martin, K. Moriarty, and S. Samuel, Columbia University report (unpublished).
⁴K. Barad, M. Ogilvie, and C. Rebbi, Phys. Lett. **143B**, 222 (1984).
⁵W. Wilcox and R. M. Woloshyn, Phys. Rev. D **32**, 3282 (1985).
⁶J. Kogut and L. Susskind, Phys. Rev. D **11**, 395 (1975); L. Susskind, *ibid.* **16**, 3031 (1977).
⁷N. Kawamoto and J. Smit, Nucl. Phys. **B192**, 100 (1981).
⁸H. Kluberg-Stern, A. Morel, O. Napoly, and B. Petersson, Nucl. Phys. **B220**, 447 (1983).
⁹M. F. L. Golterman, University of Amsterdam Report No. ITFA-85-05 (unpublished).
¹⁰J. Kogut, M. Stone, H. W. Wyld, S. H. Shenker, J. Shigemitsu, and D. K. Sinclair, Nucl. Phys. **B225**, 326 (1983).
¹¹A. Billoire, R. Lacaze, E. Marinari, and A. Morel, Nucl. Phys. **B251**, 581 (1985).
¹²See, for example, the definition of electric charge in Ref. 8.
¹³See C. Itzykson and J. Zuber, *Quantum Field Theory* (McGraw-Hill, New York, 1980), p. 160.
¹⁴M. Creutz, Phys. Rev. D **21**, 2308 (1980).
¹⁵K. G. Wilson, Phys. Rev. D **10**, 2445 (1974).
¹⁶F. S. Beckman, in *Mathematical Methods for Digital Computers*, edited by A. Ralston and H. S. Wilf (Wiley, New York,

- 1960), p. 62.
¹⁷C. Bernard, T. Draper, K. Olynyk, and M. Rushton, Nucl. Phys. **B220**, 508 (1983).
¹⁸S. Gottlieb, P. B. Mackenzie, H. B. Thacker, and D. Weingarten, Phys. Lett. **134B**, 346 (1984); C. Bernard, in *Gauge Theory on a Lattice: 1984*, edited by C. Zachos, W. Celmaster, E. Kovacs, and D. Sivers (National Technical Information Service, Springfield, VA, 1984), p. 85.
¹⁹The two- and three-point functions satisfy a sum rule $A(0,0;t_2,t_1) = G(0,t_2)$ for $t_2 > t_1$. This simple form is a consequence of our nonperiodic boundary condition in time.
²⁰This is necessary since the fluctuations in the two- and three-point functions are correlated. See P. R. Bevington, *Data Reduction and Error Analysis For The Physical Sciences* (McGraw-Hill, New York, 1969), Chap. 4 for a discussion of error propagation.
²¹See Ref. 8 and F. Gliozzi, Nucl. Phys. **B204**, 419 (1982).
²²This procedure is used as a convenient way of summarizing the low-momentum-transfer behavior of the form factor. It does not imply this is the exact functional form of the form factor. Other parametrizations such as $F(Q^2) = 1 - Q^2/a^2\lambda^2$ or $F(Q^2) = e^{-Q^2/\lambda^2 a^2}$ would give very similar results and conclusions.
²³W. R. Frazer and J. R. Fulco, Phys. Rev. **117**, 1609 (1960). See also W. G. Holladay, *ibid.* **101**, 1198 (1956).